Theoretical investigation of the effects of solvents and para-substituents

S. M. A. Ridha[a], Z. Talib Ghaleb[b], and A. Mirdan Ghaleb[a]

[a]*Department of Physics, College of Sciences, University of Kirkuk, Kirkuk, Iraq.*
e-mail: salahyagmuroglu@uokirkuk.edu.iq; abdlhadik@uokirkuk.edu.iq
[b]*Department of Chemistry, College of Science, University of Kirkuk, Kirkuk, Iraq.*
e-mail: zahra@uokirkuk.edu.iq

Received 12 February 2024; accepted 6 June 2024

The effects of halogens (F, Br, and Cl) and solvent media (acetone, ethanol, and toluene) on the structural and electronic properties of nitrobenzene compounds were investigated by combination the DFT/B3LYP and MP2 methods with 6-31 + G (d,p) basis set. The results indicate that the bond lengths between carbon-halogen atoms are increased with increased atomic size and decreased electronegativity, whereas some bond angle magnitudes are reduced than those with substitution halogens. Also, various solvent effects of studied compounds were performed with the conductor-like polarizable continuum model (CPCM) method, showing a reduction of the dipole moment by the substitution of a hydrogen atom for a ring with halogen atoms in para-position over the ring. In addition, natural bond orbitals (NBA), chemical reactivity descriptors, and the frontier molecular orbitals (FMOs) of substituted nitrobenzene were calculated. NBO analysis showed the strong interactions within a cyclic system and the fluorine atom in P-FNB is considered the best donor. Moreover, FMO analysis showed that energy band gap is related to the nature of the substituents (halogen atoms) in the para-position of the nitrobenzene compound.

Keywords: Nitrobenzene; P-halo-nitrobenzene; DFT; MP2; dipole moment; NBO; NPA; FMOs.

DOI: https://doi.org/10.31349/RevMexFis.71.010401

1. Introduction

Aromatic nitro-compounds and their derivatives are important intermediates and building blocks in the organic synthesis of drugs and perfumes, and are extensively used as explosives [1, 2]. The ease of availability of nitro compounds makes them contribute significantly to industries, *i.e.*, pharmaceuticals, pigments, and dyes [3]. Halo aromatic compounds are important intermediates in the synthesis of pharmaceuticals and agrochemicals [4, 5].

Notrobenzene and its derivatives are examples of N-substituted aromatic compounds (NACs). One of the derivatives of nitrobenzene, para-chloronitrobenzene, is used as an intermediate to prepare various derivatives, including, p-nitrophenol, p-nitroanillne, 2, 4-dinitrochlorobenzene, and 3, 4-dichloronitrobenzene [6]. In addition, the electron-withdrawing nitro groups provide the compound' resistance to typical advanced oxidativede struction techniques [7] and generally protect compounds from chemical and biological attack [1]. Therefore, understanding the mechanisms of chemical transformation of nitrocompounds is of great importance from both a fundamental and practical standpoint.

There has been extensive research involving both experimental and computational work that has studied the vibrational spectra and electronic structure properties of halogens and substituted nitrobenzene [8–13]. To our knowledge, there have been no other calculations for the effect of solvent on the electronic properties of halogens-nitrobenzene compounds by the MP2 method. Hence, we wish to investigate the electronic properties of nitrobenzene and its derivatives, para-halo-nitrobenzene (where halo=-F, -Br, -Cl), in both gas and solvents phases. The calculated Frontier Molecular Orbitals (FMOs) of title compounds also describe the molecular electronic properties in detail.

In this work, four nitro benzenes: nitrobenzene (NB), p-chloronitrobenzene (P-Cl NB), p-fluoronitrobenzene (P-FNB), and p-bromonitrobenzene (P-Br NB), were studied in gas phase and different solvents for understanding effects of solvent and substituents on the electronic structures of nitrobenzene compound.

2. Computational details

All the quantum chemical calculations were performed utilizing the Gaussian 09 program [14] with Gauss View 5.0.9 visualization [15] to study the effects of halogens (F, Br, and Cl) and solvent media (acetone, ethanol, and toluene) on the structural and electronic properties of nitrobenzene compound. Geometry optimization calculations were performed using density functional theory (DFT) [16] along with Beck's three-parameter hybrid density functional, B3LYP [17], and Moller-Plesset second-order perturbation theory (MP2) [18] on the same split-valence double zeta 6-31+G (d,p) basis set. The DFT-B3LYP method is considered one of the most used computational methods in studying compounds because its results agree with experimental results [19, 20]. The geometry optimization of the nitrobenzene and its derivatives p-halo-nitrobenzene (p-chloronitrobenzene, p-fluoronitrobenzene, and p-bromonitrobenzene) was achieved in the gas phase. The optimization procedure finds the geometry corresponding to the nearest local minimum of energy, but not necessarily the global minimum.

TABLE I. Optimized geometrical parameters of the studied compounds (bond lengths and bond angles) calculated by DFT/B3LYP and MP2 methods with same 6-31+G (d, p) basis set in gas phase.

Compounds	Bond Type	Bond Length R (Å)		Bond Type	Bond Angles A(°)	
		MP2	DFT/B3LYP		MP2	DFT/B3LYP
NB	(C-H)	1.0826	1.0829	(C1-C2=C3)	118.069	118.467
	(C-C)	1.3988	1.3989	(C6=C1-H7)	120.081	120.197
	(C=C)	1.3966	1.3947	(C1-C2-H8)	121.910	121.858
F-NB	(C-C)	1.3945	1.3963	(C1-C2=C3)	118.617	118.985
	(C=C)	1.3912	1.3926	(C6=C1-H7)	119.848	119.901
	(C-F)	1.3621	1.3516	(C1-C2-H8)	121.340	121.345
Cl-NB	(C-C)	1.3983	1.3982	(C1-C2=C3)	118.549	118.975
	(C=C)	1.3943	1.3927	(C6=C1-H7)	119.933	120.160
	(C-Cl)	1.7337	1.7494	(C1-C2-H8)	121.326	121.253
Br-NB	(C-C)	1.3982	1.3975	(C1-C2=C3)	118.404	118.783
	(C=C)	1.3945	1.3925	(C6=C1-H7)	120.147	120.282
	(C-Br)	1.8913	1.8951	(C1-C2-H8)	121.436	121.381

The Natural Bond Orbital (NBO) populations, Natural Population Analysis (NPA) [21], second-order perturbation stabilization energies E2, and dipole moments are examined at the same theoretical level to provide information on electronic structure, molecular orbitals and to understand the electronic properties, electrophilic and nucleophilic active centers in the studied compounds. The frontier molecular orbitals (FMOs) were then calculated to predict the reactivity of all studied compounds using the HOMO-LUMO gap values and with these values were calculated the chemical potential (μ), electronegativity (χ), global hardness (η), global softness (S) and electrophilicity index (ω) descriptors. Finally, in order to investigate the energetic behavior of the molecule in solvent media, the geometries of the studied compounds were optimized at the same theoretical level in three different solvents by employing the Conductor-like Polarizable Continuum Model (CPCM) [22], with dielectric constants (ε) of non-polar Toluene $(\varepsilon = 2.374)$, polar aprotic Acetone $(\varepsilon = 20.493)$, and polar protic ethanol $(\varepsilon = 24.852)$. In this model, the solvent is represented as a dielectric polarizable continuum and the solute is placed in a cavity of approximately molecular shape.

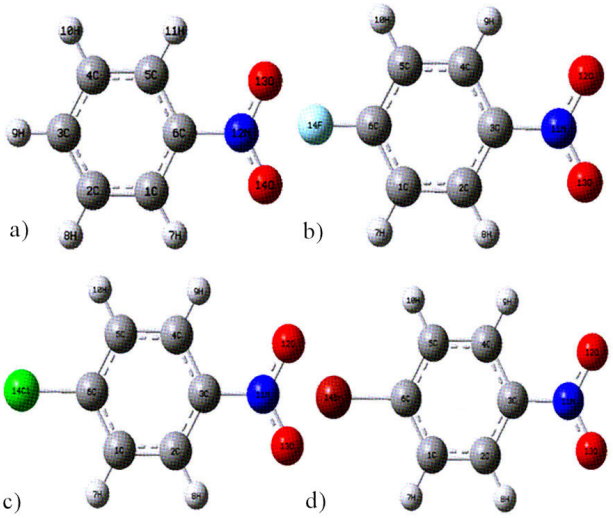

FIGURE 1. Optimized structures of a) Nitrobenzene (NB), b) para-Fluoronitrobenzene (P-FNB), c) para-chloronitrobenzene (P-ClNB), and d) para-bromonitrobenzene (P-BrNB) compounds.

3. Results and discussion

3.1. Geometrical parameters

The calculated structural properties in the gas phase of Nitrobenzene (NB) and its derivativesp-halo-nitro benzeneare summarized in Table I and Fig. 1. Table I compares theoretical calculated bond lengths and bond angles by DFT/B3LYP and MP2 with the same 6-31+G(d, p) basis set for NB, P-ClNB, P-FNB, and P-BrNB. The calculated bond lengths R and bond angles A were affected by the type of method used in the calculation. Most bond angles are extended at the DFT/B3LYP compared to those in the MP2 method. In contrast, the bond lengths have become larger in the DFT/B3LYP method for some bond lengths and become smaller for other angles.

The optimized C-C and C=C bond lengths R of NB are equal to 1.3988 Å and 1.3966 Å for the MP2 method (1.3989 Å and 1.3947 Å for DFT/B3LYP). The C-C and C=C bond lengths are reduced by replacing NB with F (P-FNB) to form a C-F bond in MP2 method and are equal to 1.3945 Å, 1.3912 Å and 1.3621 Å, respectively (1.3963 Å, 1.3926 Å, and 1.3516 Å at DFT/B3LYP). The substitution of NB by Cl (P-ClNB) reduces the bond lengths of C-C and C=C also,

TABLE II. Calculated dipole moment (M) of the studied optimized compounds (in Debye) in the studied solvent and gas phases at DFT/B3LYP and MP2 methods with the same 6-31+G (d, p) basis set.

Compound	Experimental	Gas ($\varepsilon = 1$)		Toluene ($\varepsilon = 2.374$)		Acetone ($\varepsilon = 20.493$)		Ethanol ($\varepsilon = 24.852$)	
		MP2	B3LYP	MP2	B3LYP	MP2	B3LYP	MP2	B3LYP
NB	4.22*	4.51	4.96	5.16	5.74	5.72	6.44	5.74	6.46
P-BrNB	(2.65)**	2.98	3.56	3.31	4.12	3.65	4.62	3.66	4.64
P-ClNB	(2.62)**	2.92	3.39	3.39	3.92	3.75	4.40	3.76	4.42
P-FNB	(2.57)**	2.79	3.34	3.21	3.90	3.57	4.41	3.58	4.44
MAE(Mean Absolute Error)		0.285	0.7975						

*Experimental data taken from reference [26];

**Experimental data taken from reference [27].

forming a C-Cl bond in the MP2 method and equal to 1.3983 Å, 1.3943 Å, and 1.7337 Å, respectively (1.3982 Å, 1.3927 Å, and 1.7494 Å at DFT/B3LYP). Furthermore, when NB was substituted with Br (P-BrNB), the C-C and C=C bond lengths after C-Br bond formation decreased to1. 3982 Å, 1.3945 Å, and 1.8913 Å respectively (1.3975 Å, 1.3925 Å, and 1.8951 Å at DFT/B3LYP). These statements may be due to the substitution effect of halogens (the negative inductive effect of the halogens) working to pull the electrons toward themselves. The effect of halogen (F, Cl, Br) atoms, which is small, is different from that of C-C and C=C bond lengths in NB, as shown in Table I. The bond length R for C-halogen increases with increasing atomic size and decreasing electronegativity, and the trend is as follows: R (C-Br)> R(C-Cl) > R (C-F). The bond angles magnitudes A (C1-C2-H8) and A (C6=C1-H7) are reduced than that with substitution halogens like P-FNB, P-ClNB, and P- BrNB in the following order: A (P-BrNB)>A (P-ClNB)>A (P-FNB).This behavior indicates that the most electron affinity of F is the highest compared to the electron affinity of Cl and Br [23]. Therefore, as the size of the halogen increases, the negative inductive effect of the halogen decreases. Therefore, as the size increase, the value of the bond length of the halogen increases [24].

3.2. Dipole moment

The prediction of the dipole moment M is an important issue that is related to the stability of molecules in polar environments [25]. We have studied molecular dipole moment values for four compounds (NB, P-ClNB, P-FNB, and P-BrNB) in the gas phase and in different solvents calculated on the MP2 and DFT/ B3LYP method with 6-31+ G(d,p) basis set using the NBO technique. CPCM calculations were used to predict the solvent effects on the nitrobenzene compound and its para position substituted derivatives.

The calculated dipole moments M in different solvent media (*i.e.* toluene, acetone, and ethanol) with different dielectric constant (ε) values; non-polar toluene ($\varepsilon = 2.374$), polar a protic acetone ($\varepsilon = 20.493$), and polar protic ethanol ($\varepsilon = 24.852$) are shown in Table II. One can conclude from

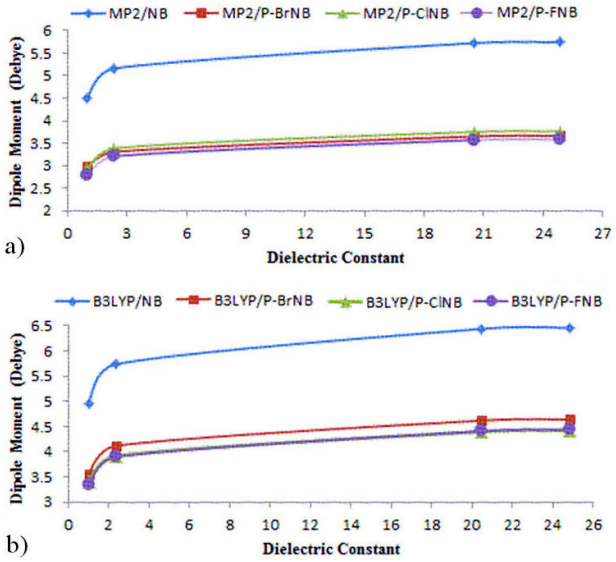

FIGURE 2. Dependence of the dielectric constant of the dipole moments of the studied compounds at a) MP2 and b) DFT/B3LYP methods with the same 6-31+G (d, p) basis set.

the data that the order of the calculated dipole moment values in all different studied environments are (M) NB>P-BrNB>P-ClNB>P-FNB. Moreover, it was noted that the mean absolute error (MAE) in dipole moments for studied compounds in the gas phase at DFT/B3LYP method is larger, 0.7975, than that for the MP2 method, 0.285, compared to the experimental data [26, 27]. The best agreement between the calculated and experimental dipole moments was obtained by MP2 method.

Among the considered compounds, the NB compound has the highest dipole moment in the solvent and gas phases considered due to its large dipole interaction. It has been noticed that the NB dipole moment is reduced by substitution of a hydrogen atom for a ring with halogen atoms in para-position over the ring. In fact, the reduction observed in the NB dipole moment on the substitution of hydrogen atom with the halogen atoms is due to the negative inductive power of the halogen atoms. For instance, the NB dipole moment in the MP2 method is 4.51 D(4.96 D at DFT/B3LYP) and in the

gas phase, is reduced to 2.79 D, 2.92 D, and 2.98 D at MP2 method (3.34, 3.39, and 3.56 D at DFT/B3LYP) when there are fluorine, chlorine, and bromine atoms in para-position, respectively.

The dipole moments calculated for the studied molecules in solvents with different polarities (ethanol $>$ acetone $>$ toluene) show that the dipole moments of the studied molecules increase as they move from the gas phase to the solvent phase, with increasing solvent dielectric constant,as shown in Fig. 2. The DFT/B3LYP calculation shows higher dipole moment values than the MP2 calculations on the same basis set. The highest dipole moment value for all the studied molecules was for ethanol. As shown in Table II, the dipole moment increases as one moves from the gas phase to a more polar solvent, with the highest dipole moment occurring for a NB compound in the ethanol solvent with a value of 5.74 D in MP2 (6.46 DinDFT/B3LYP), while compound with an F substitution (P-FNB) in gas phase has the lowest dipole moment 2.79 D at MP2 (3.3448D at DFT/B3LYP). The nature of the substituent (halogen atoms) in the para-position of the nitrobenzene compound is remarkably related to the dipole moment. In this study, the dipole moment of the nitrobenzene compound was the largest compared to P-BrNB, P-ClNB, and P-BrNB. This is a result of the fact that the direction of the dipole moment of the para functional groups (C-F, C-Cl, and C-Br) is opposite to that of the dipole moment of the nitro-functional groups; as a result, it leads to a decrease in the value of the dipole moment in the presence of these substitutions.

3.3. Natural population analysis

Natural population analysis (NPA) determines the electrons of each atom in a substance so that the weighted occupancy of the orthogonal natural orbitals is maximized. Based on the natural bond orbital (NBO), NPA is useful for understanding the role of natural atomic orbitals and their hybridization in produce chemical bonds; the use of NPA, which is the closest to a reasonable atomic population analysis method, as a default option for computational chemistry programs [28] and is likely to be widely applicable.

In the NBO technique, the electronic wave function is analyzed by Lewis and modeled under local chemical bonds. Based on the eigenvectors of the local-block single-particle density matrix, it was developed to study the hybridization and covalence of multi-atomic wave functions [29]. The NBO technique was used to study the charge distribution for compounds (NB, P-ClNB, P-FNB, and P-BrNB) in studied solvents and in the gas phase. The charge distribution of dipolar compounds in the presence of the solvent medium often undergoes significant changes [30].

The calculated atomic charges of studied compounds by NBO analysis in the gas phase and studied solve using the MP2 and DFT/B3LYP methods with 6-31+G (d, p) basis set are reported in Table III. These results can better be represented in graphical form for easier comparison as has been given in Fig. 3.

In the MP2 method for the NB compound, all carbon atoms are negative charges except for C3 which has a positive charge which may be due to its attachment with the electron-withdrawing nitro group NO2 and also indicates the charge transfer from carbon C3 to the nitro group NO2. In contrast, by the method of DFT/B3LYP, it can be observed that the carbon atom C3 has a negative charge and C6 are positive, while in the case of replacing the hydrogen atom in nitrobenzene (NB) compound with halogen atoms, para-halogen-nitrobenzene compounds, the charge on the carbon atom C6 by MP2 method is in the gas phase, for instance, is calculated to be -0.18598e (NB), -0.08945e (P-BrNB), -0.01148e (P-ClNB), and 0.51789e (P-FNB). The order of the partial charge at carbon atom C6 is NB$>$P-BrNB$>$P-ClNB$>$P-FNB. This order agrees with the chemical sense where the electron-withdrawing substituent (higher electronegativity) decreases the negative charge at this para-position. The charge C6 of para-halogen-nitrobenzene compounds possesses a lot less negative charge than other carbon atoms, this is due to the electron-withdrawing nature of the halogen atoms by means of a negative inductive effect.

Figure 3 shows the nitrogen atom N has the most positive charge whereas oxygen atoms O2 have the most negative charges. The result suggests that the atom bonded to oxygen atoms N is an electron donor and also indicates the charge transfer from the nitrogen atom N to the oxygen atoms O2. With increasing polarity, the partial charges for N and O atoms vary differently in solvents, for instance, it was observed that partial charges of O13 and N in the studied compounds steadily decreased when passing from the gas phase to a more polar solvent and in the following order: Gas$<$Toluene$<$Acetone$<$Ethanol.

In the same medium, there is no appreciable change in the partial charge on the O13 and N atoms for both the methods of the considered compounds. All hydrogen atoms in the studied molecules were found to be positive, as expected.

Table III, in the DFT/B3LYP method and in all different environments, generally, carbon atom C2 shows more negative charge for the studied compounds and in the following order: P-FNB $>$ P-ClNB$>$ P-BrNB$>$ NB. For instance, at DFT/B3LYP and MP2 methods, the partial charge on the C2 is in the range of -0.23061 to -0.29093e and -0.15215 to -0.18708e respectively, whereas there is no appreciable change in the partial charge on the C2 in the studied solvents of both methods for the considered compounds. In the MP2 method and in studying different media, the carbon atom C1 and oxygen atom O13 show more negative charge compared to the DFT/B3LYP method, for instance, in the MP2 method, the partial charges on the C1 and O13 are in the range of -0.25102 to -0.31978e (-0.18558 to -0.20963e at DFT/B3LYP) and -0.45502 to -0.48562e (-0.37905 to -0.40960e at DFT/B3LYP) respectively. The value and quality of the charge on carbon atom C3 changes significantly

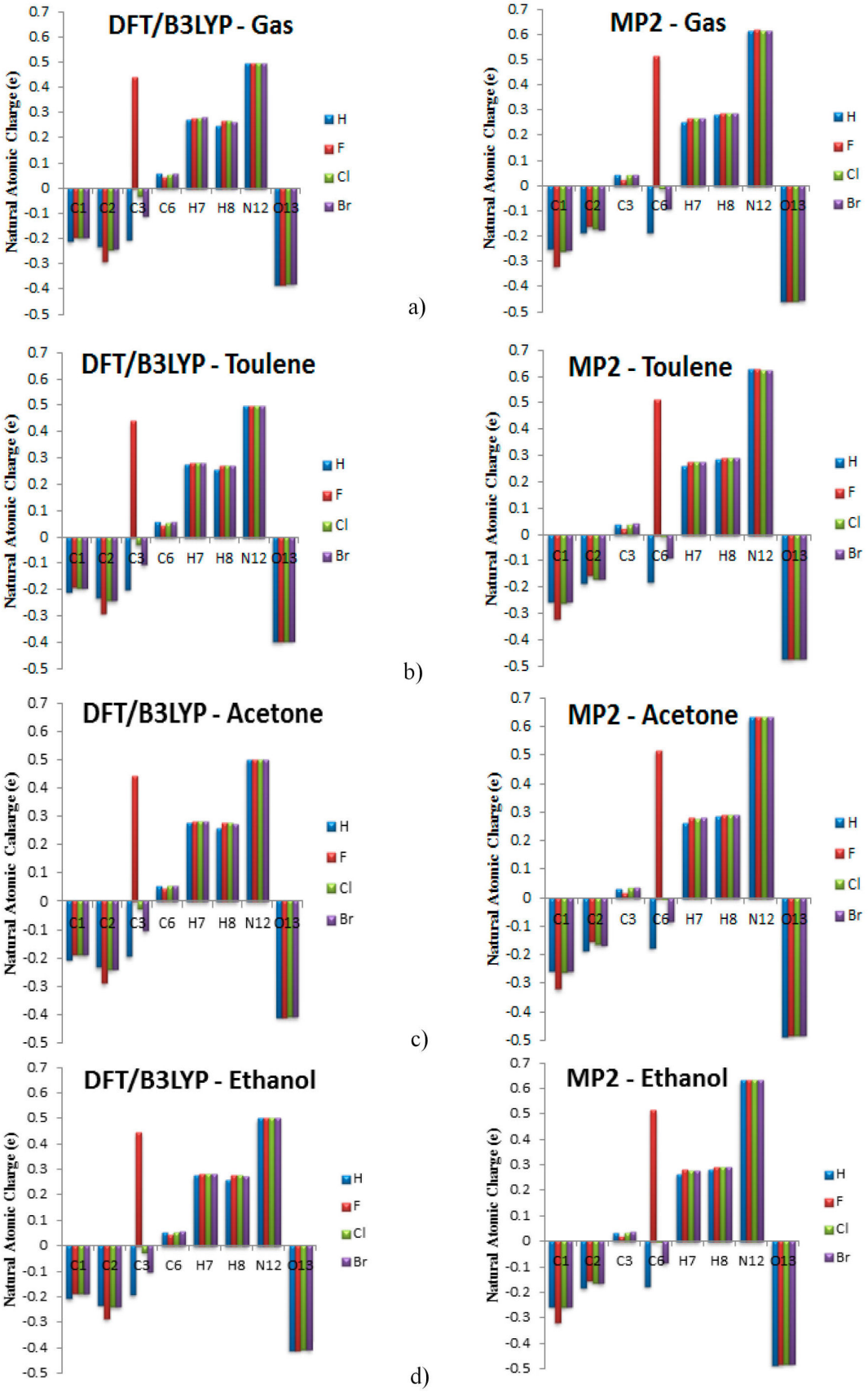

FIGURE 3. Graphical representation of the natural atomic charges for the studied compounds by DFT/B3LYP and MP2 methods with 6-31+G (d, p) basis sets in the a) gas phase, b) toluene, c) acetone, and d) ethanol.

due to the electronic effects caused by the introduction of substituents (F, Cl, and Br) at the para-position of nitrobenzene compound.

3.4. Natural bond orbital (NBO) analysis

NBO analysis provides a suitable basis for studying charge transfer or conjugating interactions in molecules and also provides an excellent method for studying intra- and intermolecular binding interactions [31]. Second-order perturbation theory provides data on electron-donor, electron-acceptor orbitals and their stabilization energy [32]. The changes in electron density "delocalization" between the filled (Lewis) donor and empty (non-Lewis) acceptor NBOs correspond to a more stable [33]. The σ and π electrons of C-C, C-H, N-H, and C-N bonds stabilize part of the ring by strong intra-molecular hyper conjugate interactions with the anti-bonding C-C, C-H, N-H, and C-N bonds [34]. In the present study, it should be noted that in Table IV, the $\sigma \rightarrow \sigma^*$ interaction has the lowest delocalization energy compared to the $\pi \rightarrow \pi^*$ interaction. Therefore, the σ bond has a higher electron density than the π bond.

From Table IV it is noted that the strong intra-molecular hyper-conjugative interaction of the C1-C2 bond is formed by the orbital overlap between the bonding orbital πC1-C2 to the corresponding anti-bonding orbital π^*C5-C6, which increases the electron density to 0.31211, resulting in a stabilization energy of 46 kcal/mol and intra-molecular charge transfer occurs and molecular stabilization takes places. Sim-

TABLE III. The calculated natural atomic charges of studied compounds by NBO technique in the studied solvents and gas phase at DFT/B3LYP (former) and MP2 (later) methods with 6-31+G (d, p) basis set.

	Substituent		C1	C2	C3	C6	H7	H8	N12	O13
Gas	H(NB)	DFT	-0.20963	-0.23061	-0.20291	0.05825	0.27409	0.24905	0.49398	-0.38078
		MP2	-0.25102	-0.18708	0.04601	-0.18598	0.25186	0.28167	0.61607	-0.45840
	F (P-FNB)		-0.19341	-0.29093	0.43870	0.04575	0.27844	0.26585	0.49380	-0.38092
			-0.31978	-0.15986	0.02475	0.51289	0.26907	0.28668	0.61725	-0.45745
	Cl (P-ClNB)		-0.19596	-0.24172	-0.03279	0.05556	0.27882	0.26464	0.49308	-0.37908
			-0.25875	-0.17061	0.04171	-0.01148	0.26673	0.28650	0.61517	-0.45548
	Br (P-BrNB)		-0.19673	-0.24085	-0.10820	0.05742	0.27924	0.26408	0.49275	-0.37905
			-0.25603	-0.17249	0.04500	-0.08945	0.26789	0.28721	0.61450	-0.45502
Toluene	H (NB)		-0.20761	-0.23131	-0.19842	0.05574	0.27533	0.25523	0.49903	-0.39616
			-0.25408	-0.18469	0.03927	-0.18106	0.25860	0.28314	0.62563	-0.47339
	F(P-FNB)		-0.18927	-0.28899	0.44085	0.04538	0.28045	0.27201	0.49846	-0.39619
			-0.31923	-0.15562	0.02133	0.51384	0.27552	0.28913	0.62655	-0.47189
	Cl (P- ClNB)		-0.19189	-0.24063	-0.02927	0.05509	0.28091	0.27052	0.49814	-0.39393
			-0.25907	-0.16644	0.03784	-0.00849	0.27307	0.28894	0.62463	-0.46976
	Br (P-BrNB)		-0.19247	-0.24010	-0.10496	0.05682	0.28129	0.26968	0.49763	-0.39398
			-0.25657	-0.16814	0.04122	-0.08645	0.27403	0.28965	0.62405	-0.46922
Acetone	H (NB)		-0.20544	-0.23111	-0.19246	0.05308	0.27575	0.26003	0.50163	-0.40926
			-0.25565	-0.18288	0.03338	-0.17548	0.26365	0.28384	0.63219	-0.48532
	F(P-FNB)		-0.18578	-0.28698	0.44373	0.04471	0.28167	0.27666	0.50143	-0.40887
			-0.31847	-0.15224	0.01831	0.51546	0.28018	0.29080	0.63309	-0.48320
	Cl (P-ClNB)		-0.18830	-0.23922	-0.02566	0.05428	0.28221	0.27497	0.50114	-0.40629
			-0.25888	-0.16294	0.03439	-0.00554	0.27771	0.29045	0.63116	-0.48085
	Br (P-BrNB)		-0.18894	-0.23888	-0.10196	0.05591	0.28258	0.27393	0.50070	-0.40636
			-0.25647	-0.16461	0.03788	-0.08363	0.27854	0.29128	0.63072	-0.48028
Ethanol	H (NB)		-0.20539	-0.23109	-0.19228	0.05301	0.27576	0.26015	0.50168	-0.40960
			-0.25568	-0.18283	0.03322	-0.17532	0.26378	0.28385	0.63234	-0.48562
	F(P-FNB)		-0.18558	-0.28686	0.44392	0.04467	0.28173	0.27690	0.50156	-0.40958
			-0.31845	-0.15215	0.01823	0.51551	0.28030	0.29083	0.63324	-0.48348
	Cl (P-ClNB)		-0.18817	-0.23921	-0.02560	0.05424	0.28224	0.27510	0.50112	-0.40662
			-0.25887	-0.16285	0.03430	-0.00546	0.27782	0.29049	0.63132	-0.48113
	Br (P-BrNB)		-0.18877	-0.23889	-0.10166	0.05588	0.28260	0.27405	0.50069	-0.40674
			-0.25647	-0.16452	0.03779	-0.08355	0.27865	0.29131	0.63088	-0.48056

TABLE IV. The MP2/6-31+G (d, p) level of theory the second-order perturbation energies E_2 (in kcal/mol) for the most important charge transfer interactions for the studied compounds in the gas phase.

Donor NBO(i)	ED(i) (e)	Acceptor NBO(j)	ED(j) (e)	Interaction type	E2 (Kcal/mol) X=H	X=F	X=Br	X=Cl
σ_{C1-C2}	1.97827	σ^*_{C3-N12}	0.07109	$\sigma_{C1-C2} \rightarrow \sigma^*_{C3-N12}$	5.63	5.41	5.41	5.41
		σ^*_{C2-H8}	0.00979	$\sigma_{C1-C2} \rightarrow \sigma^*_{C2-H8}$	1.73	1.63	1.67	1.67
		σ^*_{C6-F}	0.02178	$\sigma_{C1-C2} \rightarrow \sigma^*_{C6-F}$	-	5.22	-	-
		σ^*_{C6-Br}	0.01937	$\sigma_{C1-C2} \rightarrow \sigma^*_{C6-Br}$	-	-	5.35	-
		σ^*_{C6-Cl}	0.01805	$\sigma_{C1-C2} \rightarrow \sigma^*_{C6-Cl}$	-	-	-	5.08
π_{C1-C2}	1.64009	π^*_{C3-C4}	0.38155	$\pi_{C1-C2} \rightarrow \pi^*_{C3-C4}$	39.42	34.08	38.42	37.47
		π^*_{C5-C6}	0.31211	$\pi_{C1-C2} \rightarrow \pi^*_{C5-C6}$	46.00	53.26	48.86	49.12
σ_{C2-C3}	1.97756	σ^*_{C3-C4}	0.01862	$\sigma_{C2-C3} \rightarrow \sigma^*_{C3-C4}$	5.55	5.37	5.39	5.36
		$\sigma^*_{N12-O13}$	0.04067	$\sigma_{C2-C3} \rightarrow \sigma^*_{N12-O13}$	2.79	2.75	2.79	2.78
π_{C3-C4}	1.66256	π^*_{C1-C2}	0.29439	$\pi_{C3-C4} \rightarrow \pi^*_{C1-C2}$	43.16	47.59	43.73	44.29
		$\pi^*_{N12-O14}$	0.53714	$\pi_{C3-C4} \rightarrow \pi^*_{N12-O14}$	38.58	39.68	35.49	38.95
σ_{C5-C6}	1.98241	σ^*_{C1-C6}	0.01359	$\sigma_{C5-C6} \rightarrow \sigma^*_{C1-C6}$	2.59	3.63	3.95	4.13
		σ^*_{C5-H10}	0.00943	$\sigma_{C5-C6} \rightarrow \sigma^*_{C5-H10}$	1.43	1.48	1.80	1.67
π_{C5-C6}	1.63646	π^*_{C1-C2}	0.29439	$\pi_{C5-C6} \rightarrow \pi^*_{C1-C2}$	35.12	31.67	33.38	32.94
		π^*_{C3-C4}	0.38155	$\pi_{C5-C6} \rightarrow \pi^*_{C3-C4}$	52.51	56.27	48.26	49.53
$\sigma_{N12-O13}$	1.99545	σ^*_{C2-C3}	0.01862	$\sigma_{N12-O13} \rightarrow \sigma^*_{C2-C3}$	0.87	0.91	0.90	0.91
$\sigma_{N12-O14}$	1.99545	σ^*_{C3-C4}	0.01862	$\sigma_{N12-O14} \rightarrow \sigma^*_{C3-C4}$	0.87	0.91	0.90	0.91
$\pi_{N12-O14}$	1.99004	π^*_{C3-C4}	0.38155	$\pi_{N12-O14} \rightarrow \pi^*_{C3-C4}$	4.10	4.04	3.03	4.17
		$\pi^*_{N12-O14}$	0.53714	$\pi_{N12-O14} \rightarrow \eth^*_{N12-O14}$	5.34	5.41	5.38	5.38
LP(1)O13	1.98241	$\acute{o}^*_{C3-N12}$	0.07109	LP(1)O13$\rightarrow \acute{o}^*_{C3-N12}$	5.99	5.99	6.05	6.03
		$\acute{o}^*_{N12-O14}$	0.04067	LP(1)O13$\rightarrow \acute{o}^*_{N12-O14}$	2.59	2.62	2.61	2.63
LP(2)O13	1.93143	$\acute{o}^*_{C3-N12}$	0.07109	LP(2)O13$\rightarrow \acute{o}^*_{C3-N12}$	11.95	12.06	12.07	12.04
		$\acute{o}^*_{N12-O14}$	0.04067	LP(2)O13$\rightarrow \acute{o}^*_{N12-O14}$	24.42	24.43	24.36	24.40
LP(3)O13	1.51622	$\eth^*_{N12-O14}$	0.53714	LP(3)O13 $\rightarrow \eth^*_{N12-O14}$	259.45	259.38	260.37	260.11
LP(1)O14	1.98241	$\acute{o}^*_{N12-O13}$	0.04067	LP(1)O14$\rightarrow \acute{o}^*_{N12-O13}$	2.59	2.62	2.61	2.63
		$\acute{o}^*_{C3-N12}$	0.07109	LP(1)O14$\rightarrow \acute{o}^*_{C3-N12}$	5.99	5.99	6.05	6.03
LP(2)O14	1.93143	$\acute{o}^*_{C3-N12}$	0.07109	LP(2)O14$\rightarrow \acute{o}^*_{C3-N12}$	11.95	12.06	12.07	12.04
		$\acute{o}^*_{N12-O13}$	0.04067	LP(2)O14$\rightarrow \acute{o}^*_{N12-O13}$	24.42	24.43	24.36	24.40
LP(3)F	1.91686	$\eth^*_{C5-C6}$	0.34065	LP(3)F$\rightarrow A^*_{C5-C6}$	-	22.86	-	-
LP(3)Br	1.91962	$\eth^*_{C5-C6}$	0.36373	LP(3)Br$\rightarrow A^*_{C5-C6}$	-	-	15.01	-
LP(3)Cl	1.91678	$\eth^*_{C5-C6}$	0.36506	LP(3)Cl$\rightarrow A^*_{C5-C6}$	-	-	-	18.71

ilarly, $\pi \rightarrow \pi^*$ interactions occur between the bond πC1-C2 and the anti-bonding orbital π^*C3-C4, and between the bond πN12-O14 and the anti-bonding orbital π^*C8-N10, increasing the electron density by 0.38155 and 0.53714, respectively, and stabilizing each bond at 39.42 (strong) and 5.34 kcal/mol (weak) respectively. Moreover, it is noted that the maximum occupancies 1.97827, 1.97756, 1.98241, 1.99545, and 1.99004 are obtained for σ (C1-C2), σ (C2-C3), σ (C5-C6), σ(N-O), and π(N-O) respectively. Therefore, the results suggest that the σ (C1-C2), σ(C2-C3), σ(C5-C6), σ(N-O), and π(N-O) are mainly controlled by the p character of the hybrid orbitals. The NBO analysis also describes the bonding in terms of the natural hybrid orbitals, highlighting that the LP(3) O13 has the lowest occupancy (1.51622e) and the strongest stabilizing interaction. Thus, the electron donation to the π^*N12-O14 anti-bonding orbital of the LP(3) O13 $\rightarrow \pi^*$N12-O14 interaction involves an orbital very close to the pure p-type lone-pair orbital, in the considered compounds as evident from Table IV. Clearly, the donor-acceptor LP(3) O13$\rightarrow \pi^*$N12-O14 interaction shows the largest stabilization energy and this is due to the stability of the resonance within the nitro group. From our analysis, the most important intra-molecular hyper conjugative interactions resulted in the highest stabilization energies of

TABLE V. Global reactivity descriptors calculated for nitrobenzene and its para-substituted derivatives at MP2 and DFT/B3LY methods with the basis set 6-31+G (d,p).

Compound		Parameter										
		HOMO (eV)	LUMO (eV)	ΔE (eV)	μ (eV)	η (eV)	ω (eV)	S (eV)	χ (eV)	$\Delta N_{\max}$ (eV)	IP (eV)	EA (eV)
Gas												
NB	MP2	-10.0865	0.7493	10.8358	-4.6686	5.4179	2.0114	0.1845	4.6686	0.8616	10.0865 (9.86)*	-0.7493
	DFT	-7.5826	-4.0788	3.5038	-5.8307	1.7519	9.7028	0.5708	5.8307	3.3282	7.5826	4.0788
P-FNB	MP2	-10.5301	0.6489	11.179	-4.9406	5.5895	2.1835	0.1789	4.9406	0.8839	10.5301	-0.6489
	DFT	-8.0096	-4.2290	3.7805	-6.1193	1.8903	9.9048	0.5290	6.1193	3.2372	8.0095	4.2290
P-ClNB	MP2	-10.2631	0.5031	10.7662	-4.88	5.3831	2.2119	0.1857	4.88	0.9065	10.2631	-0.5031
	DFT	-7.9714	-4.2505	3.7209	-6.1109	1.8605	10.0362	0.5375	6.1109	3.2846	7.9714	4.2505
P-BrNB	MP2	-10.1249	0.4585	10.5834	-4.8332	5.2917	2.2072	0.1889	4.8332	0.9133	10.1249	-0.4585
	DFT	-7.9552	-4.2445	3.7106	-6.0998	1.8553	10.0274	0.5389	6.0998	3.2877	7.9551	4.2445
Toluene												
NB	MP2	-9.9529	0.6849	10.6378	-4.634	5.3189	2.0186	0.1880	4.634	0.8712	9.9529	-0.6849
	DFT	-7.4311	-4.2292	3.2017	-5.8301	1.6009	10.6163	0.6246	5.8301	3.6418	7.4310	4.2292
P-FNB	MP2	-10.385	0.6315	11.0165	-4.8767	5.5082	2.1588	0.1815	4.8767	0.8853	10.385	-0.6315
	DFT	-7.8406	-4.3299	3.5106	-6.0852	1.7553	10.5482	0.5697	6.0852	3.4667	7.8405	4.3299
P-ClNB	MP2	-10.1396	0.4944	10.634	-4.8226	5.317	2.1870	0.1880	4.8226	0.9070	10.1396	-0.4944
	DFT	-7.8060	-4.3454	3.4606	-6.0757	1.7303	10.667	0.5779	6.0757	3.5113	7.8060	4.3454
P-BrNB	MP2	-10.0063	0.4546	10.4609	-4.7758	5.2304	2.1803	0.1911	4.7758	0.9130	10.0063	-0.4546
	DFT	-7.7935	-4.3435	3.4500	-6.0685	1.7250	10.6744	0.5797	6.0685	3.5179	7.7935	4.3435
Acetone												
NB	MP2	-9.8525	0.6127	10.4652	-4.6199	5.2326	2.0394	0.1911	4.6199	0.8829	9.8525	-0.6127
	DFT	-7.3078	-4.3735	2.9342	-5.8406	1.4671	11.6258	0.6816	5.8406	3.9809	7.3077	4.3735
P-FNB	MP2	-10.2403	0.6016	10.8419	-4.8193	5.4209	2.1422	0.1844	4.8193	0.8890	10.2403	-0.6016
	DFT	-7.7138	-4.4249	3.2888	-6.0693	1.6444	11.2006	0.6081	6.0693	3.6908	7.7137	4.4249
P-ClNB	MP2	-10.0487	0.4683	10.517	-4.7902	5.2585	2.1818	0.1901	4.7902	0.9109	10.0487	-0.4683
	DFT	-7.6811	-4.4374	3.2437	-6.0592	1.6219	11.3187	0.6165	6.0592	3.7360	7.6811	4.4374
P-BrNB	MP2	-9.9162	0.4345	10.3507	-4.7408	5.17535	2.1714	0.1932	4.7408	0.9160	9.9162	-0.4345
	DFT	-7.6710	-4.4377	3.2332	-6.0543	1.6166	11.3369	0.6185	6.0543	3.7450	7.6710	4.4377
Ethanol												
NB	MP2	-9.8501	0.6106	10.4607	-4.6197	5.2303	2.0402	0.1911	4.6197	0.8832	9.8501	-0.6106
	DFT	-7.3048	-4.3773	2.9274	-5.8410	1.4637	11.6544	0.6831	5.8410	3.9905	7.3047	4.3773
P-FNB	MP2	-10.2367	0.6008	10.8375	-4.8179	5.4187	2.1418	0.1845	4.8179	0.8891	10.2367	-0.6008
	DFT	-7.7073	-4.4303	3.2768	-6.0688	1.6384	11.2395	0.6103	6.0688	3.7040	7.7072	4.4303
P-ClNB	MP2	-10.0465	0.4674	10.5139	-4.7895	5.2569	2.1818	0.1902	4.7895	0.9110	10.0465	-0.4674
	DFT	-7.6778	-4.4412	3.2366	-6.0595	1.6183	11.3445	0.6179	6.0595	3.7443	7.6778	4.4412
P-BrNB	MP2	-9.914	0.4337	10.3477	-4.7401	5.1738	2.1714	0.1932	4.7401	0.9161	9.914	-0.4337
	DFT	-7.6689	-4.4407	3.2281	-6.0548	1.6141	11.3565	0.6195	6.0548	3.7512	7.6688	4.4407

*Experimental data are taken from [40].

46 kcal/mol, 43.16 kcal/mol, and 52.51 kcal/mol were obtained for $\pi_{C1\text{-}C2} \rightarrow \pi^*_{C5\text{-}C6}, \pi_{C3\text{-}C4} \rightarrow \pi^*_{C1\text{-}C2}$, and $\pi_{C5\text{-}C6} \rightarrow \pi^*_{C3\text{-}C4}$ of NB respectively, while 53.26 kcal/mol, 47.59 kcal/mol, and 56.27 kcal/mol for P-FNB respectively, 48.86 kcal/mol, 43.73 kcal/mol, and 48.26 kcal/mol for P-BrNB respectively, 49.12 kcal/mol, 44.29 kcal/mol, and 49.53 kcal/mol for P-ClNB, respectively, as shown in Table IV. These strong interactions within a cyclic system in-

dicate a highly delocalized structure, and additional stability was also observed for the substituted chlorine, fluorine, and bromine atoms resulting from the stability of the resonance. This stability is due to the reverse flow from the lone pairs of halogen atoms to the aromatic ring via the pi-pair electrons. These results indicate that the stability energies of the studied nitrobenzene derivatives are of the following order: P-FNB>P-ClNB>P-BrNB. This means that the stability energy is directly proportional to the electronegativity. From the NBO analysis, it is inferred that the substituted fluorine atom is the most activated of the substituted halogens. This activation may be due to the fact that 2p orbital of fluorine overlaps well with the p orbital of the pi-system, resulting in a stronger pi-bond [35]. This can be demonstrated by comparing the stability energies of the non-bonding interactions of the studied para-halo-nitrobenzene compounds. For example, the P-FNB compound has the largest non-bond interaction corresponding to LP(3) F$\rightarrow \pi^*$(C5-C6) with a stabilization energy of 22.86 kcal/mol, while the stabilization energy for the LP(3) Br$\rightarrow \pi^*$C5-C6 of the P-BrNB compound is 15.01 kcal/mol whereas the LP(3) Cl$\rightarrow \pi^*$(C5-C6) for P-ClNB compound the stabilization energy is 18.71 kcal/mol. Therefore, the fluorine atom in P-FNB is considered the best donor because it has the highest non-bounding interaction.

3.5. Frontier molecular orbital (FMO) analysis

One of the simplest methods to compute the excitation energies is calculating the difference between the Frontier Molecular Orbital (FMO) energies (HOMO-LUMO energy gap). FMO analysis is greatly used to explain the electronic and optical properties of organic compounds [36]. Therefore, we calculated the HOMO and LUMO energies, energy band gap (ΔE), chemical potential (μ), hardness (η), softness (S), electrophilicity index (ω), electronegativity (χ), the maximum electronic charge $(\Delta N_{\max})$, ionization potential (IP), and electron affinity (EA) for the title compounds in all media using DFT/B3LYP and MP2 methods with 6-31G+(d,p) basis set. The computed global reactivity descriptors for the studied compounds listed in Table V are in all studied media.

Knowledge of HOMO and LUMO energies is very important for measuring the chemical reactivity of molecules. The energy gap of FMOs determines molecular electrical transport [37] and explains the deducing intra-molecule charge transfer interaction. Molecules with large energy gaps are less chemically reactive and more kinetically stable [38–40]. This is because removing an electron from the HOMO, which has a small energy gap, and adding an electron to the LUMO, which has a large energy gap, is energetically undesirable. For example, a molecule with a large energy gap is stable and therefore is chemically harder than another molecule with a smaller energy gap [41]. Therefore, as indicated by Table V, the P-FNB compound which has the highest energy band gap is harder and more stable (less reactive), while the NB compound with the lowest energy band gapis softer and least stable of all (more reactive) in all different media. The energy band gap for the NB compound substituted with halogen atoms (F, Cl, and Br) is increased when increasing the electronegativity of substituted atoms in DFT/B3LYP and MP2 methods, *i.e.*, there is a proportional relation between the energy band gap and electronegativity of substituted atoms.

One can conclude from the data that the order of the calculated energy band gap values in all different studied environments is P-FNB $>$ P- ClNB$>$ P-BrNB. In this study, the energy band gap decreased on going from the gas phase to a more polar solvent, with the highest energy gap occurring for compound (P-FNB) in gas phase with a value of 11.179 eV at MP2 method (3.7805 eV at DFT/B3LYP), while compound with a Br substitution (P-BrNB) in ethanol solvent has the lowest energy gap 10.3477 eV at MP2 (3.2281 eV at DFT/B3LYP). The energy band gap is notably related to the influence of the substituent (halogen atom) at the para position of the nitrobenzene compound. In a comparison between the MP2 and DFT/B3LYP methods for all studied compounds, the DFT/B3LYP calculation shows higher HOMO energy and lower LUMO energy than the MP2 calculation. For example, the HOMO energy of the NB compound in the gas phase is in the range of (-10.0865 to -10.5301 eV) and in the range (-7.5826 to -8.0096 eV) by the MP2 and DFT/B3LYP methods, respectively, and the LUMO energyis in the range of (0.7493 to 0.4585 eV) and (-4.0788 to -4.2505 eV) by the MP2 and DFT/B3LYP methods, respectively. For all title compounds, MP2 calculations showed a significantly larger energy band gaps than the DFT/B3LYP Method. For example, the energy band gap values for the P-ClNB compound are in the range of (3.2366 to 3.7209 eV) and (10.5139 to 10.7662 eV) for the DFT/B3LYP and MP2 methods, respectively. Furthermore, the MP2 method,which calculates the ionization potential (IP) of NB compound in the gas phase, which depends directly on the HOMO energy, is closer to the experimental data than the DFT/B3LYP method: the experimental IP energy of NB compound [42] is 9.86 eV, while the MP2 method is 10.0865eV, DFT/B3LYP method predicted 7.5826 eV. With reference to these results, the MP2 method, which estimates the IP of the NB compound, is in good agreement with the experimental data, in contrast to the DFT/B3LYP method.

The electrophilicity index (ω) defined by Parr *et al*. [43] is the stabilization energy that the system obtains when it gains enough electrons to saturate. It is therefore a measure of a system's ability to accommodate additional electrons and is defined as follows:

$$\omega = \frac{\mu^2}{2\eta},$$

where μ represents the electronic chemical potential and η is the global chemical hardness. These parameters are often approximated through frontier orbital energies, which describe charge transfer within a system in the ground state, leading to:

$$\mu \cong \frac{(E_{HOMO} + E_{LUMO})}{2},$$
$$\eta \cong \frac{(E_{LUMO} - E_{HOMO})}{2},$$

where E_{HOMO} and E_{LUMO} are the energies of the highest occupied and lowest unoccupied molecule orbitals (HOMO and LUMO), respectively [44]. From these results, it is clear that the NB compound has the highest reactivity and the P-FNB compound has the lowest reactivity. It can be noticed that the presence of fluorine atom at the para-position of nitrobenzene molecule improves the charge transfer within the molecule ($\mu = -5.8307$ to -6.1193 eV at DFT/B3LYP and -4.6686 to -4.9406 eV at MP2). Also, the obtained results show that the P-FNB compound has higher electronegativity (χ) *i.e.* strongly electrophilic and has higher charge flow, whereas the NB compound is nucleophilic (see Table V). Furthermore, $\Delta N_{\max}$ represents the maximum electronic charge, S is the global softness and χ denotes the absolute electronegativity, which is a good measure of a molecule's ability to attract electrons to itand is used to calculate the direction of electron migration, given by

$$\Delta N_{\max} = -\frac{\mu}{\eta}, \quad S = \frac{1}{\eta}, \quad \chi = (IP + EA)/2.$$

Here, EA(-LUMO) and IP(-HOMO) are the electron affinity and ionization potential, respectively; larger valuesof EA indicate higher electrophilicity and smaller values of IP indicate higher nucleophilicity.

In this study, Quantum chemical calculations for the EA (Table V), larger differences between the different MP2 and DFT/B3LYP methods were found. Moreover, all studied compounds have positive EA at the DFT/B3LYP method and create stable anions whereas, in the MP2 method,they have negative EA and create unstable anions. Even if the anion is stable, the electronic state may be very diffuse. Therefore, the EA cannot be expected to be as accurate as the IP calculation [45].

As shown in Table V, the effect of the substitution atoms on the values of the HOMO and LUMO energies in the studied compounds. Halogen atoms lead to a decrease in the frontier molecular orbital energy. It is noted that the NB compound has HOMO energy of -7.5826 eV at DFT/B3LYP (-10.0865 eV at MP2), and F, Cl, Br-para substituted derivatives (electron-withdrawing atoms) have the HOMO energies of -8.0096, -7.9714, and -7.9552 eV at DFT/B3LYP method, respectively, and in contrast, -10.5301, -10.2631, and -10.1249 eV at MP2 method, respectively. It is clear that using the halogen substituents stabilizes the HOMO energy levels. In the solvents and gas phases, all the studied compounds have positive $\Delta N_{\max}$ values and act as electron acceptors from their environment. Moreover, due to the large HOMO-LUMO energy gap, the global hardness and stability of the studied compounds increase as follows: P-FNB $>$ P-ClNB$>$ P-BrNB$>$ NB, while the chemical reactivity decreases in the reverse order: P-FNB $<$ P-ClNB$<$ P-BrNB$<$ NB.

4. Conclusion

In this study, the optimized geometries calculated at the MP2 and DFT/B3LYP methods with the same 6-31+G (d, p) basis set in the gas phase of Nitrobenzene (NB) and its derivatives (P-FNB, P-ClNB, and P-BrNB) and showed that the most bond angles are extended at the DFT/B3LYP compared to those at the MP2 method. In contrast, the bond lengths became larger in the DFT/B3LYP method for some bond lengths and became smaller for another angle. The bond lengths (R) of C-halogens are increased with increasing atomic size and decreasing electronegativity, and the magnitudes of some bond angles were smaller than for substituted halogens. According to the calculations of the two methods above show that the dipole moment of the studied molecules increases as the dielectric constant of the solvent increases as it moves from the gas phase to the solvent phase. On the other hand, due to the negative inductive power of the halogen atom, the dipole moment decreases as the hydrogen atom on the ring is replaced by a halogen atom in the para-position and the best agreement between calculated and experimental dipole moments was obtained using the MP2 method. Natural Population Analysis (NPA) of atomic charges shows that the negative charge on the carbon atom of the nitrobenzene derivatives replaced by halogen atoms at the para-site decreases with the increase in the electronegativity of the halogen atoms (electron-withdrawing substituent). In addition, the impact of electronic effects resulting from the induction of substituents (F, Cl, and Br) at the para-position of nitrobenzene compound causes a significant change in the value and quality of the charge on the carbon atom attached to the nitro (NO2) group. NBO analysis showed the strong interactions $(\pi_{C-C} \rightarrow \pi^*{}_{C-C})$ within a cyclic system indicate a highly delocalized structure and additional stability was also observed for the substituted fluorine, chlorine, and bromine atoms resulting from the stability of the resonance and the fluorine atom in P-FNB is considered the best donor because it has the highest non-bonding interaction. FMO analysis shows that the energy band gap decreases from the gas phase to more polar solvents, with the highest energy gap occurring for compound (P-FNB) in gas phase, while compound with a Br substitution (P-BrNB) in ethanol solvent has the lowest energy gap. The energy band gap is influenced by the nature of the substituent (halogen atom) at the para-position of the nitrobenzene compound. Furthermore, due to the large HOMO-LUMO energy gap, the global hardness and the stability of the studied compounds increase in the following order: P-FNB $>$ P-ClNB$>$ P-BrNB$>$ NB, and the chemical reactivity decreases in the opposite order: P-FNB $<$ P-ClNB$<$ P-BrNB$<$ NB. In addition, it is found that the MP2 method in estimating the IP energy of the NB compound is in good agreement with the experimental data in contrast to DFT/B3LYP.

1. K.-San Ju and R. E. Parales, Nitroaromatic Compounds, from Synthesis to Biodegradation, *Microbiol. Mol. Biol. Rev.* **74** (2010) 250. https://doi.org/10.1128/mmbr.00006-10.
2. J. Moon *et al*., Site-selective and metal-free C-H nitration of biologically relevant N-heterocycles, *Archives of Pharmacal Research* **44** (2021) 1012, https://doi.org/10.1007/s12272-021-01351-5.
3. Y. Kumar, S. Rani, J. Shabir, and L. S. Kumar, Nitrogen-Rich and Porous Graphitic Carbon Nitride Nanosheet-Immobilized Palladium Nanoparticles as Highly Active and Recyclable Catalysts for the Reduction of Nitro Compounds and Degradation of Organic Dyes, *ACS Omega* **5** (2020) 13250, https://doi.org/10.1021/acsomega.0c01280.
4. R. O. M. A. de Souza, L. S. M. Miranda, and U. T. Bornscheuer, A retrosynthesis approach for biocatalysis in organic synthesis, *Chem. Eur. J.* **23** (2017) 12040, https://doi.org/10.1002/chem.201702235.
5. S. A. Shepherd *et al*., Extending the biocatalytic scope of regiocomplementary flavin-dependent halogenase enzymes, *Chem. Sci.*, **6** (2015) 3454, https://doi.org/10.1039/C5SC00913H.
6. P. K. Arora and H. Bae, Toxicity and microbial degradation of nitrobenzene, monochloronitrobenzenes, polynitrobenzenes, and pentachloronitrobenzene, *J. Chem.* **2014** (2014) 265140, https://doi.org/10.1155/2014/265140.
7. A. Gooch, N. Sizochenko, B. Rasulev, L. Gorb, and J. Leszczynski, In vivo toxicity of nitroaromatics: A comprehensive quantitative structure-activity relationship study, *Environ. Toxicol. Chem.* **36** (2017) 2227, https://doi.org/10.1002/etc.3761.
8. G. Shakila, H. Saleem, and Sundaraganesan, FT-IR, FT-Raman, NMR and U-V spectral investigation: Computation of vibrational frequency, chemical shifts and electronic structure calculations of 1-bromo-4-nitrobenzene, *World Scientific News* **61** (2017) 150.
9. S. Seshadri, R. Sangeetha, Rasheed M. P., M. Padmavathy, Molecular structure, spectroscopic (FT-IR, FT-Raman, NMR, UV), HOMO-LUMO Analysis of 1-Bromo-4-Nitrobenzene by Quantum Copmutational Methods, *IRJET* **3** (2016) 691.
10. V. Arjuman, S. T. Govindaraja, S. Sakiladevi, M. Kalaivani, and S. Mohan, Spectroscopic, electronic structure and natural bond orbital analysis of Ofluoronitrobenzene and p-fluoronitrobenzene: a comparative study, Spectrochim. *Acta Part A: Mol. Biomol. Spectrosc.* **84** (2011) 196, https://doi.org/10.1016/j.saa.2011.09.029.
11. V. Dayakumar, S. Periandy, M. Karabacak, and S. Ramalingam, Experimental (FT-IR, FT-Raman) and theoretical (HF and DFT) investigation and HOMO and LUMO analysis on the structure of p-fluoronitrobenzene, *Spectrochim. Acta Part A: Mol. Biomol. Spectrosc.* **83** (2011) 575, https://doi.org/10.1016/j.saa.2011.09.008.
12. V. Krishnakumar, N. Jayamani, and R. M. Mathammal, Density functional theory calculations and vibrational spectra of p-bromonitrobenzene, *J. Raman Spectrosc.* **40** (2009) 936, https://doi.org/10.1002/jrs.2203.
13. B.-D. Lee and M.-J. Lee, Prediction of hydroxyl substitution site(s) of phenol, monochlorophenols and 4-chloronitrobenzene by atomic charge distribution calculations, *Bull. Korean Chem. Soc.* **30** (2009) 787, https://doi.org/10.5012/bkcs.2009.30.4.787.
14. C. Moller and M. S. Plesset, Note on an approximation treatment for many-electron systems, *Phys. Rev.* **46** (1934) 618, https://doi.org/10.1103/PhysRev.46.618.
15. M. J. Frisch *et al.*, Gaussian 09, Revision A.02. Gaussian, Inc, Wallingford (2009).
16. R. Dennington, T. Keith, and J. Millam, Gauss view, version 5. Semichem Inc., Shawnee Mission. (2009)
17. A. D. Becke, Density-functional exchange-energy approximation with correct asymptotic behavior, *Phys. Rev. A* **38** (1988) 3098, https://doi.org/10.1103/PhysRevA.38.3098.
18. C. Lee, W. Yang, and R. G. Parr, Development of the Colle-Salvetti correlation-energy formula into a functional of the electron density, *Phys. Rev. B* **37** (1988) 785, https://doi.org/10.1103/PhysRevB.37.785.
19. S. M. A. Ridha, Z. T. Ghalib, and A. M. Ghaleb, The computational investigation of IR and UV-Vis spectra of 2-isopropyl-5-methyl-1,4-benzoquinone using DFT and HF methods, *East Eur. J. Phys.* **1** (2023) 197, https://doi.org/10.26565/2312-4334-2023-1-26.
20. M. En-Nylly *et al.*, Performance evaluation and assessment of the corrosion inhibition mechanism of carbon steel in HCl medium by a new hydrazone compound: Insights from experimental, DFT and first-principles DFT simulations, *Arabian Journal of Chemistry* **16** (2023) 104711, https://doi.org/10.1016/j.arabjc.2023.104711.
21. A. E. Reed, R. B. Weinstock, and F. Weinhold, Natural population analysis, *J. Chem. Phys.* **83** (1985) 735, https://doi.org/10.1063/1.449486.
22. V. Barone, and M. Cossi, Quantum calculation of molecular energies and energy gradients in solution by a conductor solvent model, *J. Phys. Chem. A.* **102** (1998) 1995, https://doi.org/10.1021/jp9716997.
23. J. E. Huheey, E. A. Keiter, R. L. Keiter, and O. K. Mehdi, Inorganic chemistry: principles of structure and reactivity. (Pearson Education India, 2006).
24. S. Ramalingam, S. Periandy, B. Elanchezhian, and S. Mohan, FT-IR and FT-Raman spectra and vibrational investigation of 4-chloro-2-fluoro toluene using ab initio HF and DFT (B3LYP/B3PW91) calculations, *Spectrochim. Acta Mol. Biomol. Spectrosc.* **78** (2011) 429, https://doi.org/10.1016/j.saa.2010.11.005.
25. A. Shiroudi *et al.*, DFT study on tautomerism and natural bond orbital analysis of 4-substituted 1,2,4-triazole and its derivatives: solvation and substituent effects *J. Mol. Model.* **26** (2020) 57, https://doi.org/10.1007/s00894-020-4316-9.

26. C. Desfrançois *et al*., Electron binding to valence and multipole states of molecules: Nitrobenzene, para- and metadinitrobenzenes, *J. Chem. Phys*. **111** (1999) 4569, https://doi.org/10.1063/1.479218.

27. A. C. Littlejohn and J. W. Smith, 483. The Dipole Moments of Some Aromatic Nitro-compounds in relation to the Steric Inhibition of the Mesomeric Effect of the Nitro-group, *J. Chem. Soc.* (1957) 2476, https://doi.org/10.1039/jr9570002476.

28. B. D. Dunnington and J. R. Schmidt, Generalization of natural bond orbital analysis to periodic systems: applications to solids and surfaces via planewave density functional Theory, J. Chem. Theory Comput. 8 (2012) 1902, https://doi.org/10.1021/ct300002t.

29. A. E. Reed, L. A. Curtiss and F. Weinhold, Intermolecular interactions from a natural bond orbital, donor-acceptor viewpoint, *Chem. Rev.*, **88** (1988) 899-926. https://doi.org/10.1021/cr00088a005.

30. V. Brenner, E. Gloaguen, M. Mons, Rationalizing the diversity of amideamide H-bonding in peptides using the natural bond orbital method, Physical Chemistry Chemical Physics, *Royal Society of Chemistry* **21** (2019) 24601, https://doi.org/10.1039/c9cp03825f.

31. J. D. Mottishaw et al., Electrostatic Potential Maps and Natural Bond Orbital Analysis: Visualization and Conceptualization of Reactivity in Sanger's Reagent, *J. Chem. Educ*. **92** (2015) 1846, https://doi.org/10.1021/ed5006344.

32. R. Gangadharan, S. Sampath Krishnan, Natural bond orbital (NBO) population analysis of 1-Azanapthalene-8-ol, *Acta Phys. Pol. A* **125** (2014), https://doi.org/10.12693/aphyspola.125.18.

33. S. Subashchandrabose, V. Thanikachalam, G. Manikandan, H. Saleem, and Y. Erdogdu, Synthesis and spectral characterization of bis(4-amino-5-mercapto- 1,2,4-tiazol-yl) propane, Spectrochim. *Acta Part A: Mol. Biomol. Spectrosc.* **157** (2016) 96, https://doi.org/10.1016/j.saa.2015.12.005.

34. H. S. Bazzi, A. Mostafa, S. Y. Alqaradawi, El-Metwally Nour, Synthesis and spectroscopic structural investigations of the charge-transfer complexes formed in the reaction of 2,6-diaminopyridine with-acceptors TCNE, chloranil, and DDQ, *J. Mol. Str.* **842** (2007) 1, https://doi.org/10.1016/j.molstruc.2006.12.005.

35. D. Durga Devi, S. Manivarman and S. Subashchandrabose, Synthesis, molecular characterization of pyrimidine derivative: A combined experimental and theoretical investigation, *Karbala Int. J. Mod. Sci.* **3** (2017) 18, https://doi.org/10.1016/j.kijoms.2017.01.001.

36. M. B. Smith, Jerry. March, March's Advance Organic Chemistry Reactions, Mechanisms, and Structure, Six Ed. (John Wiley & Sons, Inc. Hoboken, New Jersey, 2007) p. 692.

37. L. Padmaja et al., Density functional study on the structural conformations and intramolecular charge transfer from the vibrational spectra of the anticancer drug combretastatin-A2, *J. Raman Spectrosc.* **40** (2009) 419, https://doi.org/10.1002/jrs.2145.

38. S. Seshadri, M. P. Rasheed, and R. Sangeetha, Vibrational spectroscopic (FT-IR and FT-Raman) studies, HOMO LUMO analysis and electrostatic potential surface of 2-amino-4, 5-dimethyl-3-furancarbonitrile, *IOSR J. Appl. Chemistry* **15** (2015) 87, https://doi.org/10.9790/5736-088287100.

39. J. Aihara, Reduced HOMO-LUMO Gap as an Index of Kinetic Stability for Polycyclic Aromatic Hydrocarbons, *J. Phys. Chem. A* **103** (1999) 7487, https://doi.org/10.1021/jp990092i.

40. D. E. Manolopoulos, J. C. May and S. E. Down, Theoretical studies of the fullerenes: C34 to C70, *Chem. Phys. Lett.* **181** (1991) 105, https://doi.org/10.1016/0009-2614(91)90340-F.

41. Y. Ruiz-Morales, HOMO-LUMO Gap as an Index of Molecular Size and Structure for Polycyclic Aromatic Hydrocarbons (PAHs) and Asphaltenes: A Theoretical Study. I, *J. Phys. Chem. A* **106** (2002) 11283, https://doi.org/10.1021/jp021152e.

42. D. R. Lide, Handbook of chemistry and physics, (84th edition, CRC Press, Boca Raton, 2004).

43. R. G. Parr, L. Von Szentpaly, S. Liu, Electrophilicity Index, *J. Am. Chem. Soc.* **121** (1999) 1922, https://doi.org/10.1021/ja983494x.

44. R. G. Parr, R. G. Pearson, Absolute hardness: companion parameter to absolute electronegativity, *J. Am. Chem. Soc.* **105** (1983) 7512, https://doi.org/10.1002/chin.198413001.

45. H. S. Smalo, P.-O. Astrand, and S. Ingebrigtsen, Calculation of Ionization Potentials and Electron Affinities for Molecules Relevant for Streamer Initiation and Propagation, IEEE Transactions on Dielectrics and Electrical Insulation 17 (2010) 3, https://doi.org/10.1109/TDEI.2010.5492245.